12th Scientific/Research Symposium with International Participation
„METALLIC AND NONMETALLIC MATERIALS“ B&H, 19th-20th April 2018

COMPARISON OF DIFFERENT STEEL TYPES BY USING 3D TOMOGRAPHY

Emina Vardo
University of Zenica, Faculty of Metallurgy and Technology
Travnička cesta 1, Zenica
Bosnia and Herzegovina

Jessica Gola, Frank Mücklich
Saarland University, Institute of Functional Materials
Campus D3.3, Saarbrücken
Germany

Keywords: dual phase steel, tomography, serial sectioning, 3D

ABSTRACT

The results of two light optical tomographies (LOT) of two-phase steels are presented and compared in this paper. Two-phase steels show a microstructure consisting of a carbon-rich second phase and a ferritic matrix. In this work, microstructures are compared with a martensitic and a bainitic second phase. Tomographies are very important for material simulation and classification of different steels in 3D.

Serial sectioning is composed of two steps that are constantly repeated until achiving required depth. The first step is contained of polishing and etching- where a constant depth of material removal between each section is desirable. The second step is collecting two dimensional (2D) images, after each section. After collection, images are aligned and converted to binary images with image processing programs and reconstructed as a virtual 3D structure. Different parameters (e.g. the connectivity of the phase, number of particles etc.) can be measured using 3D reconstruction.

1. INTRODUCTION

In the last four decades, several new steel types have been developed and presented as a group Advanced High-Strength Steels (AHSS). Steels in this group are multiphase steels consist of hard phases of martensite, bainite and/or retained austenite in a ductile ferittic matrix. One of the most important AHSS is the Dual-Phase (DP) steel. First DP steel (back in the 1970s) showed greater formability than conventional steels and since then production of DP steel increased every year. Great mechanical properties e.g. high ultimate tensile strength, high work hardening rate, good ductility, uniform elongation and fatigue resistance, high energy absorption capacity are achieved with the microstructure consisting of a ferrite matrix and dispersed hard martensite/bainite phases. The variations of mechanical properties are achieved by controlling carbon content and with addition of alloying elements (e.g. manganese, chromium, vanadium, molybdenium, nickel etc.)

The simplest way to get ferittic-martensite steel (DP) is intercritical annealing of a ferritic-pearlitic microstructure in two-phase field ($\alpha+\gamma$) and then rapid cooling enabling transformation austenite to martensite, [1, 2, 3]. Geometrical arrangement of martensite in a

martensite-ferrite dual-phase (DP) steel affects on deformation and fracture behavior, the volume fraction of martensite and grain size. When ferrite is surrounded by honeycombed martensite fracture mode becomes brittle, while uniform elongation is higher when martensite is dispersed around ferrite. These variations are related to the tense incompatibility between ferrite and martensite [4, 5].
Ferritic-bainitic steels are subgroup of the DP steels. Bainite can be obtained by isothermal transformation at all temperatures where the formation of pearlite and proeutectoid ferrite is slow and below the martensite start temperature. For the bainite transformation also, imposition of slow cooling rate during controlled rolling process is suitable [1, 6].

In material science morphology of microstructure has a key role on properties of the material. A lot of microstructural features in 2D [7] is possible to characterize using standard microscopy instrumentation, while there are many of them that can only be measured in 3D e.g. the true size, shape, distribution of both individual phases and their local neighborhood, determining the connectivity between phases on networks and counting of the number of particle per unit volume [8, 9]. Usually information obtained from 2D images are not enough for getting real 3D microstructure properties, because of that for models, simulations and correlations, it is very important to connect standard metallography with 3D data. One of the most used metallographic devices is Light Optical Microscope (LOM). With this device is possible to examine a microstructure of materials. As it is known, microstructure represents a connection between material production and properties. In order to enhance steel desing, it is necessarily to properly understand the influences of production conditions on the microstructural state on the one side and the ways in which microstructures determine material properties, on the other side. By using only 2D images, a complete dimension of information is not taken in consideration during analyses, because they are usually performed on 2D areas obtained by cutting through the 3D material structure [10, 11]. The effect of this reduction of information is described below.

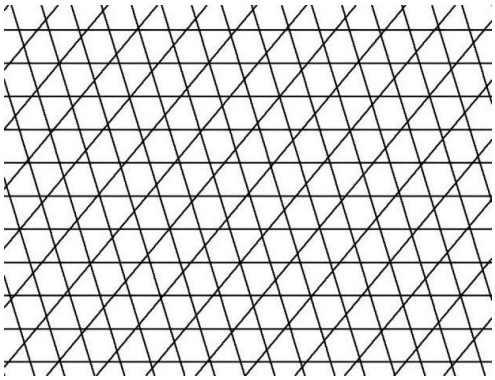

Figure 1. 2D cut through an unknown simple 3D structure [10]

In Figure 1 is displayed the planar structure emerging by a random cut through a simple 3D structure. It is very difficult to deduce or even imagine the original spatial structure from which the projection emerged and it is impossible to reconstruct it with certainty without further information. The image has emerged from a random cut through a 3D structure of stacked cubes that is displayed in Figure 2. The surface shown in Figure 1 is outlined. Although artificially constructed, this example demonstrates how distorted and misleading the view on structures can become by ignoring a spatial dimension.
In order to gain reliable information of 3D properties of microstructural constituents from 2D analysis, it is necessary to know their general shape characteristics beforehand. The

constituents may also not have a concave geometry, because otherwise they could be cut multiple times by a single plane and appear as separate constituents without connection. As an additional constraint due to practical reasons, the general shape of constituents has to be isometric, because non-isometric bodies display a much larger statistical variety of appearances for different 2D cuts [12].

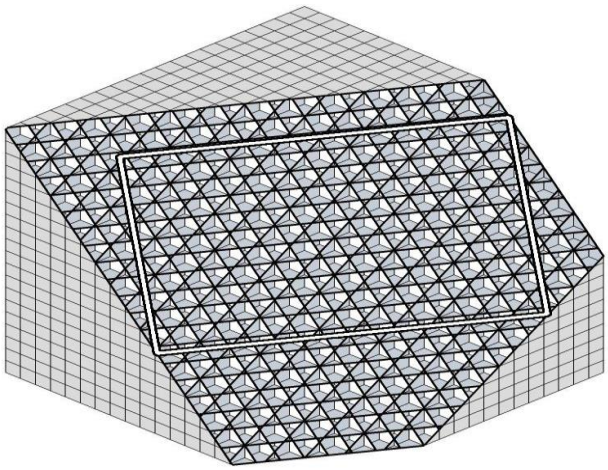

Figure 2. 2D cut through a simple 3D structure [10]

Additional to the general deficient capability of data gained from 2D structures to represent 3D properties, additional loss of information can be introduced by the utilized analysis methods. A good example is the line segment analysis [13], which is a common technique mainly used for the determination of the mean grain-size. It is based on the measurement of line segment lengths, i.e. 1D measurement data.
Due to the ever tighter tolerance ranges for the material properties of modern steels, it is therefore essential to describe the microstructures accurately. For the quantitative analysis and classification of microstructures it is of great interest to understand the correltations of parameters across all scales and dimensions. For example, new approaches in microstructure classification work with methods of computer science, the data mining methods, in combination with morphological parameters in order to achieve an objective classification of steel microstructures [14]. 3D morphological data can be used to gain new insights into the real structure with information of shape, distribution and connectivity of different phases. These information will help to detect the differences of phases, esypecially in the differentiation of martensite and bainite. Furthermore the correlations of 2D and 3D parameters can be found and further improve the data mining models. In addition, it is also possible to use these tomographies for simulations of material properties in material development [15]. With the help of simulation new steels with tailored properties can be developed more efficiently and cost-effectively.

2. EXPERIMENTAL

2.1. Material and Preparation of the samples

Samples used in this work were from steel plates with a carbon content of approximately 0.06 wt.% and two-phase microstructures consisting of a ferritic matrix and either a martensitic or a bainitic second phase. Initially, the samples were cut so that the size of the first sample was 3 x 2 x 9.5 mm^3 and of the second sample was 2 x 2 x 10 mm^3.
Before padding the samples with resin, two marks were applied to the sample in order to find the same spot for tomography again. These were later also used to align the microscope

images (Figure 3). Resin used for this purpose is EpoFix, Struers. Padding the sample should prevent edge rounding and make it possible to use the sample holder. To avoid air bubbles the resin was 24 h under vacuum. Then, sample was fixed on sample holder. Previously, the sample had to be aligned so that the microscope could capture the previously determined image area. Before the tomography could be started the sample had to have a flat surface. For that purpose grinding papers Si-C (320, 600, 1200, 2400 µm) were used.
The polishing suspension MasterPrep (MP) with 0.05 µm diamond grains was used on a neoprene cloth to avoid scratches during the tomography.

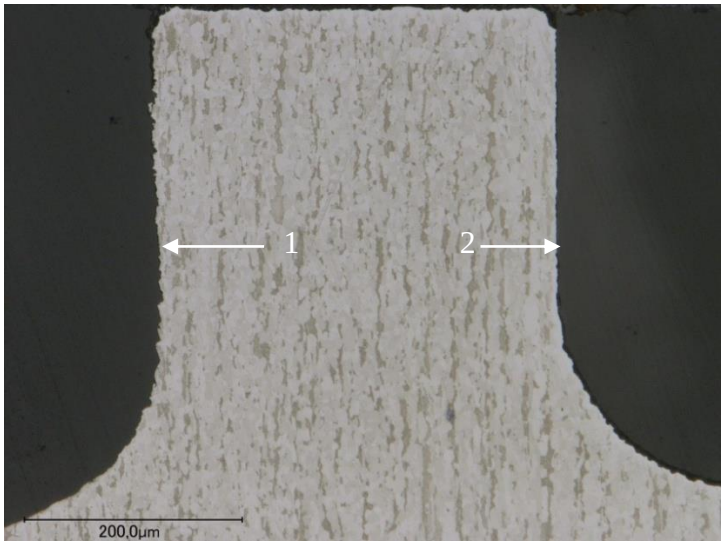

Figure 3. Image of the etched martensitic structure, two marks used to align the microscope images can be seen

2.2. Etching
For reconstruction it is important that the phases can be separated from each other in the light microscope images, Figure 4a) and 4b).

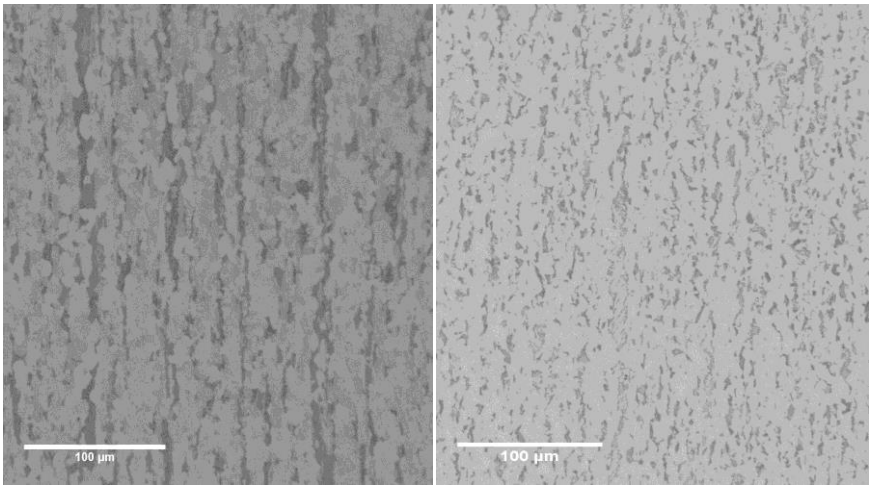

a) *b)*

Figure 4. Light optical images of the etched microstructure, a) for the martensitic sample and b) for the bainitic sample

For this reason, the samples were etched with a modified Beraha etching solution consisting of 3 g of potassium metabisulphite and 100 ml of deionized water to contrast the second phase in the ferrite matrix. Beraha solution was added drop by drop between 25-40 s. The advantage of the Beraha etching in combination with a short etching time is that no structure appears on the matrix and the second phase objects can be nicely visualized and appear dark in the light microscope [15].

2.3. Microscopy

After samples were prepared serial sectioning could start. Experimental setup for serial sectioning was based on the previous thesis of J. Webel [17]. The images were made with Leica TXP microscope with Keyence VH-Z250R optics and magnification of 500, as presented on the Figure 3. Size of the images was 1600 x 1200 pixels with a pixel size of 409 nm x 409 nm. Stereomicroscope of the Leica TXP was removed and replaced by the Keyence VH-Z250R optics, because stereomicroscope was on long distance from the surface of the sample with the small magnification. The new Keyence optics had to be mounted perpendicular to the polishing plane and could be moved above the sample for taking images. The advantages were minimization of insertion and removal errors and considerable time saving in the preparation of the tomography.

2.4. Serial sectioning

During the whole serial sectioning the sample was fixed on the sample holder in TXP. In this work desired depth was 125 μm for both tomographies. The following steps were repeated until the desired depth was reached:

- Polishing,
- cleaning (water, ethanol and isopropanol) and drying with pressurized air,
- etching,
- cleaning (ethanol and isopropanol) and drying with pressurized air,
- image recording.

For the first tomography 380 cuts (one cut was contained of all these steps) were made and 243 for the second. Difference in number of cuts was mostly because of the size of the sample, polishing force, polishing time and amount of suspension.

2.5. 3D-Reconstruction and analysis

Before 3D-reconstruction was possible these several steps had to be done:

- alignment,
- segmentation,
- removing errors with MATLAB script,
- 3D-analyse and vizualisation.

First two steps were done in Software Amira and the last step in Software Mavi and Amira.
With the help of the reconstruction program Amira the images of light optical microscope were aligned. Each image was aligned with the one below it. The image was moved and rotated until markings in both images come to the same position. Figure 5a) shows two consecutive LOM images of the bainitic tomography which are not aligned with each other. The marks (dark frame) are offset to each other. The upper picture is displayed transparently in order to be able to cover fixed markings such as marks by shifting and twisting. As shown

in Figure 5b), the superimposed view shows that the structures that have been superimposed are uniformly grey.
In this way, aligned stacks were obtained which correctly reflect the development of the sample structure in the volume.

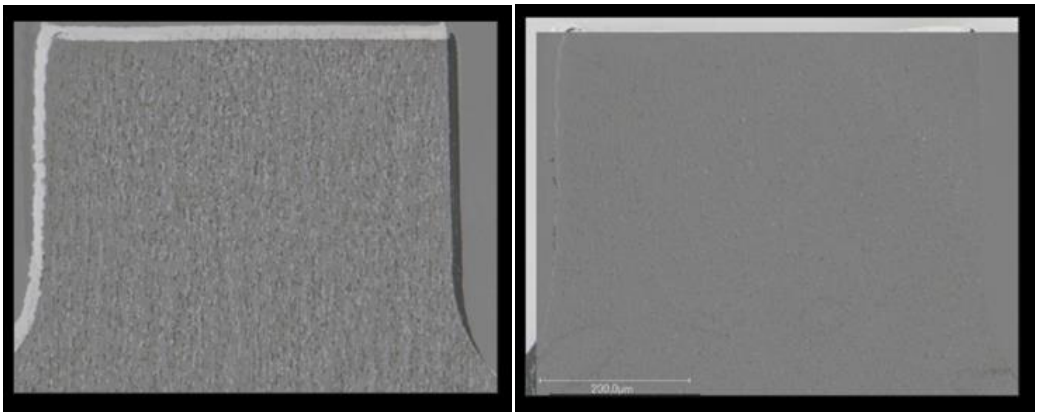

a) *b)*

Figure 5. a) Two consecutive LOM images of the bainitic tomography before superimposition in the reconstruction program Amira. The brighter, transparent image 1 is superimposed on the upper slice by moving and twisting the image 2 (transform upper slice) by superimposing the marks in both images, b) Overlay of two consecutive LOM images from the bainitic tomography. The border of the black frame visible in Figure 6 can hardly be seen in the superimposition

After alignment, image stacks were cropped to the desired size. In the next step, the LOM images that represent the 3D image stack were segmented by threshold. Areas containing martensite or bainite were white, all other areas were segmented in black. Due to Beraha etching, the areas of the substructure were darker than the ferrite areas. Figure 6 shows the result of segmentation with subsequent binarization as an example for the tomographies of the two available samples. The areas of the substructure have the gray value 1 after binarization, all other areas have the gray value 0. Artefacts of the segmented images were removed by a MATLAB script that deleted all white objects that are only present in a single slice.

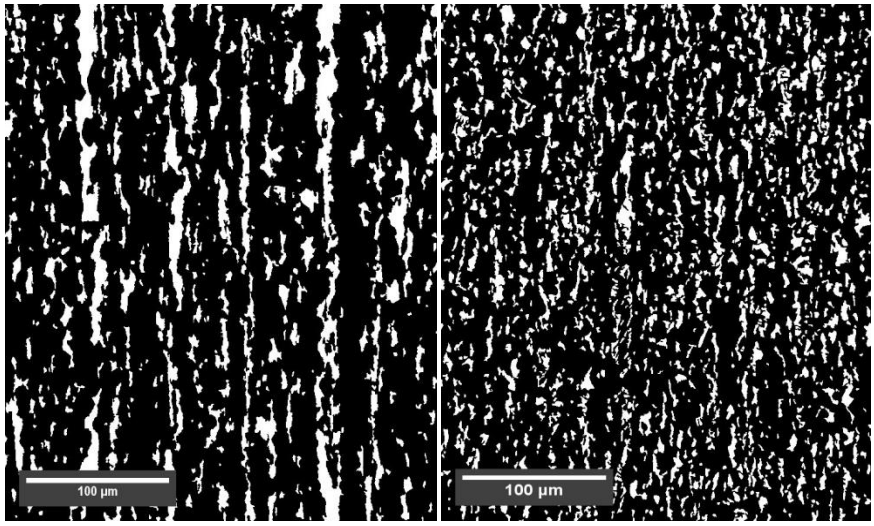

a) *b)*

Figure 6. After binarization following segmentation of the light optical microscopy images using Amira, the areas of the substructure appear white while the surrounding ferrite matrix is displayed as black a) for segmentation of martensitic tomography and b) segmentation of bainitic tomography

The alignment can be described as the foundation stone of the reconstruction. The sample volume can only be realistically mapped by precisely aligning the consecutive 2D images. This ensures that the calculations following the reconstruction can be transferred to the original sample. The 3D analysis of the previously reconstructed data sets was carried out with the MAVI program. Of interest were the so-called field and object parameters of the tomographies, which contain various information such as the volume, the surface, the Euler number of the second phase objects and much more. To determine these, the light optical microscopy image set was loaded into the program and scaled according to the pixel size (409 nm for x and y). Then 3D parameters: volume, surface, Euler number and number of particles of the tomography were measured.

For visualisation the individual second phase objects of the tomography were separated from each other in the program and labelled separately. Unconnected objects appeared in different colors as shown in Figure 7.

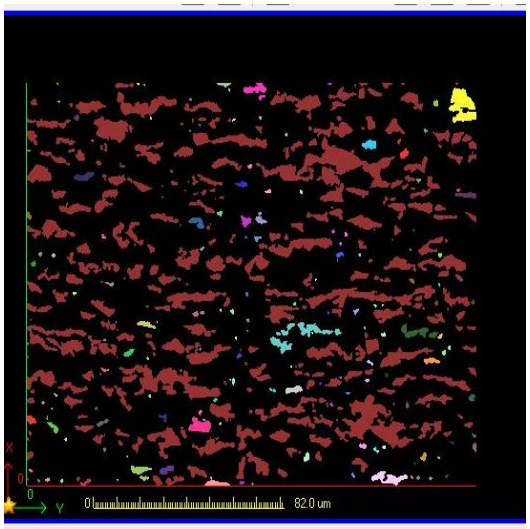

Figure 7. Slice view of the bainitic tomography in Mavi. The second phase objects of the displayed sample volume appear in different colors. Objects of the same color are connected in volume.

3. RESULTS AND DISCUSSION

Removal of the material

In order to obtain isotropic voxel, the resolution in z-direction should be in the same range as the pixel size. For this reason, a parameter optimization study was first carried out to obtain the desired removal rate. As shown in Figure 8, the removal is changed using varying parameters. In the beginning, the speed of the polishing disk was 300 RPM, polishing time 2 minutes, amount of polishing suspension was 2 ml, force was 10-18 and material removal was in average 0.249 nm (from 0 to 34th cut). In this area of the curve in the Figure 8 some inhomogeneities can be seen. They are probably caused by wrong magnification.

In order to increase removal from 35th to 200th cut, force was increased on 15-25, but removal still was too low, in average 0.267 nm. Then it was noticed that polishing suspension was not applied on the right way. So with this properly applying of suspension and polishing time of 3 minutes, material removal, from 201th to 270th cut, was increased to 0.327 nm. This removal still was not enough, so the next step was to increase speed to 400 RPM and force to 25-30. With these changes, material removal, from 271th cut to 380th cut, was in average 0.453 nm.

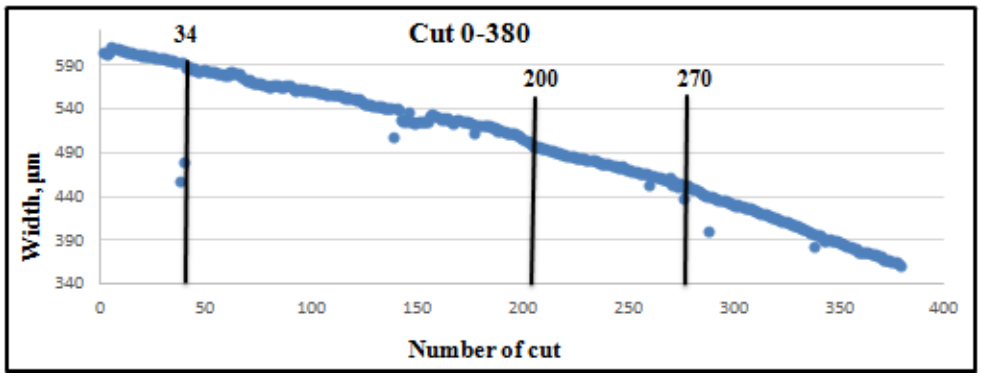

Figure 8. Material removal per cut, martensitic tomography

With low force removal of the material was insufficient on the other hand high force causes scratches on the surface, so it was necessary to find optimum force range considering the type of the steel and speed of the polishing disk. Constant amount of the polishing suspension was very important because then amount of diamond grains on polishing disk was constant which causes the same material removal through whole tomography. It was noticed during this tomography also that short polishing time as a result has insufficient material removal.

The bainitic tomography was carried out with the optimized parameters (polishing time was 3 minutes, speed of the polishing disk was 400 RPM, force was in average 30 and it was used 2 ml of polishing suspension per cut). Because of these parameters, there were constant throughout the tomography, material removal was constant, in average 0.466 nm per cut, (Figure 9).

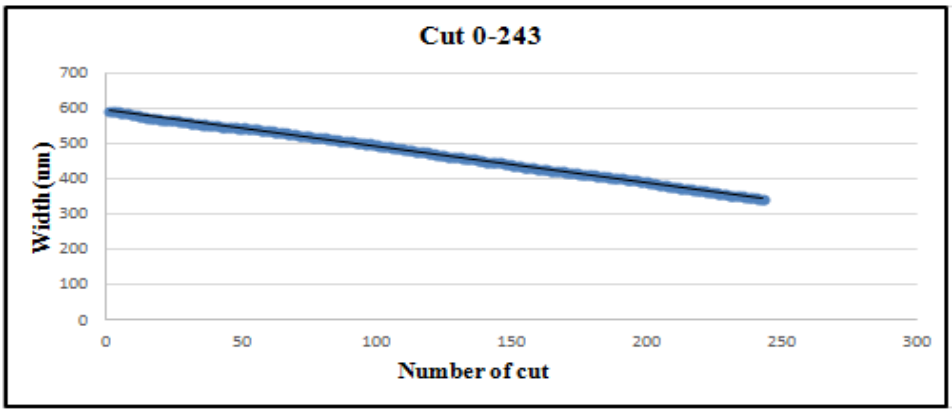

Figure 9. Material removal per cut, bainitic tomography

Visualization

Visualization enabled the 3D representation of the various tomography datasets. To visualize the tomography, the images labelled by MAVI were used. Objects of the same color were linked in volume. Figure 10a) is the visual representation of the martensitic sample and b) of the bainitic sample. Due to the coloring, it is now visible which second phase objects are connected. As it can be seen in Figure 10a) and 10b), rolling direction is in Z direction for both tomographies.

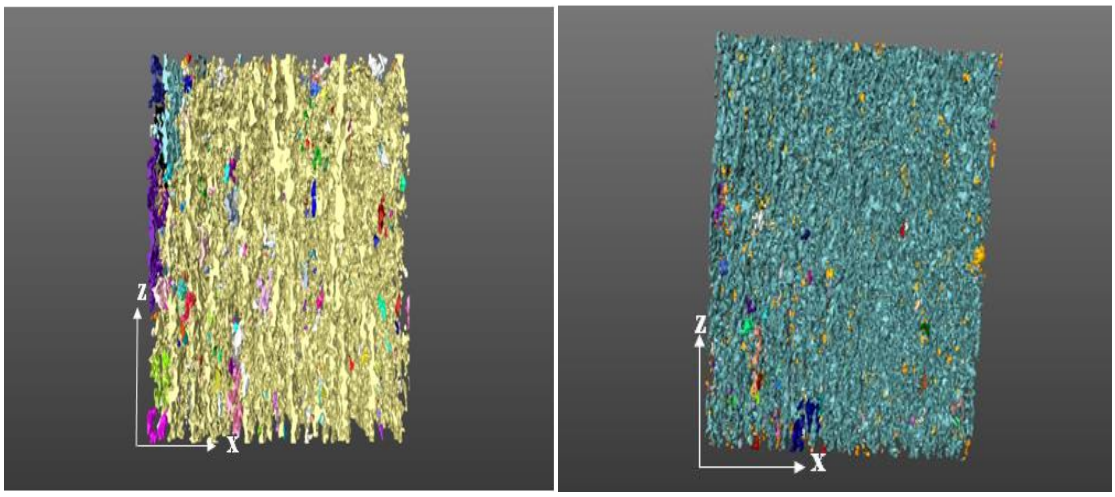

Figure 10. a) Visualisation of the martensitic tomography in XZ plane and b) visualization of the bainitic tomography in XZ plane

3D Measurements

Table 1 shows the results of the 3D measurements with MAVI for both samples.

Table 1. Analyses of the structural parameters for the first and second tomography

	Martensitic tomography	**Bainitic tomography**
Total volume (µm³)	300x334x125	296x386x125
Volume/porosity	0.8217	0.8062
Volume/volume density	0.1783	0.1938
Surface/surface	2.84E-06	4.53E-06
Surface/surface density	231900	317954
Integral of Total Curvature/ Euler number	-18615	-59518
Integral of Total Curvature/Euler density	-1.53E+15	-4.21E+15
Number of particles	10827	20132
Particles density	8.64E-04	14.09E-04

The total volume of the martensitic tomography was 12325000 µm³, and volume density was 0.1783 that means martensite had a volume fraction of 17.83% of the total volume. The negative Euler number suggested that martensite grains have a lot of holes. For the bainitic tomography total volume was 14282000 µm³ with a volume fraction of bainite of 19.38%

In comparison, it could be seen that bainitic tomography showed a 2% higher volume fraction of the second phase than martensitic tomography. However, the surface area in 3D for martensitic tomography was about twice as large as that of bainitic tomography, which also lead to a higher surface density for this tomography. The visual impression of a finer distribution of the second phase could be measured by the particle density parameter. Bainitic tomography had twice as many particles as martensitic tomography and the particle density was 63% higher for bainitic tomography.

4. CONCLUSION

In the present work, two serial sectional tomographies were performed on two micro-alloyed steels. The first 3D microstructure tomography had a martensitic second phase with a total volume of 300 x 334 x 125 μm^3 and the second tomography had a volume of 296 x 386 x125 μm^3 with a bainitic second phase. The cutting distance of the tomographies was smaller than 500 nm. For the constant removal of the material it was very important to keep all parameters of tomography constant (speed of the polishing disk, force, time, amount of suspension etc.). The best way to achieve that is to do few trial sections to check removal before tomography begins. If only one parameter is changed during the tomography it will effect on the result.
One things which can also be conclude is the size of the sample that has a very important role in the tomography. With smaller sample size, removal of the material is faster.
Visualization of the tomography illustrates the importance of 3D microstructure analysis because single particles which can be seen in 2D actually are connected through the volume.

5. REFERENCE

[1] Tsipouridis P.: "Mechanical properties of Dual Phase steels", Doctoral dissertation, München, 2006.,

[2] Brands D., Balzani D., Scheunemann, L., Schröder, J., Richter H., Raabe D.: "Computational modeling of dual-phase steels based on representative three-dimensional microstructures obtained from EBSD data", 2015.,

[3] Khedkar P., Motagi R., Mahajan P., Makwana G.: "A Review on Advance High Strength Steels", International Journal of Current Engeneering and Technology, vol. Special Is, no. 6, , pp. 240–243, 2016.,

[4] Sato N., Adachi Y., Kawata H., Kaneko K.: "Topological Approach to Ferrite/Martensite Dual-phase microstructures" ISIJ International, Vol. 52 (2012).,

[5] Tasan C. C., Diehl M., Yan D., Bechtold M., Roters F., Schemmann L., Zheng C., Peranio N., Ponge D., Koyama M., Tsuzaki K., Raabe D.: "An Overview of Dual-Phase Steels: Advances in Microstructure-Oriented Processing and Micromechanically Guided Design", Annual Review of Material Research., vol. 45, no. 1, pp. 391-431, 2014.,

[6] Bhadeshia H.K.D.H.: "Bainite in Steels", third ed., IOM Communication Ltd., The Institute of Materials, London, 2001.,

[7] Ohser J., Mücklich F.: "Statistical Analysis of Microstructures in Materials Science" Karlsruhe, Saarbrücken, (2001).,

[8] DeHoff R.T.: "Quantitative serial sectioning analysis" , J Microsc 131:259–263, 1983.,

[9] Wolfsdorf T.L., Bender W.H., Voorhees P.W.: "The morphology of high volume fraction solid liquid mixtures: an application of microstructural tomography", 1997.,

[10] Fischer M., Stieben A., Quade H., Bleck W.: "3D Metallography of a Multiphase steel", 26. Aachener Stahlkolloquium, 2011.,

[11] Turner D.M., Kalidindi S.R.: "Statistical construction of 3-D microstructures from 2-D exemplars collected on oblique sections", Acta Materialia 102 (2016) 136-148.,

[12] Velichko A., Mücklich F.: "Quantitative 3D-Gefügeanalyse-Sterologieoder Tomographie", Praktische Metallographie 45 (2008) 9, S. 423-439.,

[13] DIN EN ISO 643:2003-09,

[14] Gola J., Britz D., Staudt T., Winter M., Schnieder A.S., Ludivici M., Mücklich F.: „Advanced microstructure classification by data mining methods", Comput Mater Sci. – accepted, 2018.,

[15] Scherff F., Goldschmidt F., Scholl S., Diebels S: „High-resolution simulation of microstructures in dual-phase steel" Pamm, 2016.,

[16] Britz D., Hegetschweiler A., Roberts M. and Mücklich F.: "Reproducible Surface Contrasting and Orientation Correlation of Low-Carbon Steels by Time-Resolved Beraha Color Etching", Materials Performance and Characterization, Vol. 5, No. 5, 2016, pp. 553–563, http:/ / dx.doi.org/ 10.1520/ MPC20160067. ISSN 2165-3992,

[17] Webel J.: „Methodische Entwicklung eines Verfahrens zur seriellen Schnitttechnik für lichtmikroskopische Materialtomographien", 2013.